The Effect of Fluoride and Iron Content on the Clinkering of Alite-Ye'elimite-Ferrite (AYF) Cement Systems

Visa Isteri[1], Katja Ohenoja[2], Theodore Hanein[3], Hajime Kinoshita[3], Mirja Illikainen[2], Pekka Tanskanen[1] and Timo Fabritius[1]*

[1]Process Metallurgy, Faculty of Technology, University of Oulu, Oulu, Finland, [2]Fibre and Particle Engineering, Faculty of Technology, University of Oulu, Oulu, Finland, [3]Department of Materials Science and Engineering, The University of Sheffield, Sheffield, United Kingdom

Alite–ye'elimite–ferrite (AYF) cement is a more sustainable alternative to Portland cement (PC) that may offer improved mechanical, rheological, and chemical performance. Using traditional raw materials and conventional clinker processing conditions, alite (C_3S) and ye'elimite ($C_4A_3\$$), the major phases in PC and calcium sulfoaluminate (CSA) cements, respectively, cannot be coproduced. The typical formation temperature in the kiln for alite is >1350°C, but ye'elimite normally breaks down above 1300°C. However, with careful composition control and in the presence of fluoride, alite can be mineralized and formed at lower temperatures, thus enabling the production of AYF clinkers in a single stage. In this study, the production of AYF cement clinkers with different chemical compositions is attempted at 1250°C. The sensitivity of the fluoride content is initially assessed with a fixed target clinker composition to determine the optimal requirements. The effect of altering the target ferrite (C_4AF) and alite (C_3S) contents is also assessed followed by the effect of altering the target C_4AF and $C_4A_3\$$ contents. It is shown that AYF clinkers can be produced in a single stage through the careful control of the fluoride content in the mix; however, the formation/persistence of belite and mayenite could not be avoided under the conditions tested. It is also shown that ~10 wt% ferrite in the target composition provides sufficient AYF clinker burnability and the amount of fluoride needs to be controlled to avoid stabilization of mayenite.

Keywords: calcium sulfoaluminate cement, alite and belite, fluoride, waste valorization, alternative cement binder, low-carbon cement

INTRODUCTION

Concrete is the most used building material worldwide, and its production is rising due to population growth and urbanization. Concrete consists of aggregates, water, and a binder/cement; the global production of cement for concrete is approximately 4 billion tons (Cembureau, 2019). The most used binder is Portland cement (PC), the production of which, due to large demand, is a major contributor to global CO_2 emissions that are threatening human life on Earth. The majority of these emissions are from the calcination of limestone (mostly $CaCO_3$) to obtain calcium oxide (CaO), which is a key ingredient in cement clinker production. The second major contributor is the burning of fossil fuels

required to reach clinkering temperature. PC is usually produced at ~1450°C, which is required for the formation of the main clinker mineral, alite (C₃S[1]) that is only thermodynamically stable above 1250°C (Hewlett et al., 2019; Hanein et al., 2020) but starts to form in industrial kilns at temperatures >1350°C (Telschow, 2012). The CaO content of clinkers needs to be reduced to minimize the chemical CO_2 required for clinkering, while the process energy needs to be minimized to reduce the CO_2 emissions stemming from fossil fuel combustion. Raw-material CO_2 reduces when lower CaO-bearing phases are used in the order of $C_4A_3\$ < C_4AF < C_3A < C_2S < C_3S$ (Gartner, 2004; Barcelo et al., 2014).

Alite–ye'elimite–ferrite (AYF) cement can combine the favorable characteristics of PC and ye'elimite-rich cements. AYF is an alternative/modified PC in which all the tricalcium aluminate (C_3A) and some of the other clinker phases are replaced with ye'elimite ($C_4A_3\$$); thus, it requires less calcareous source in the raw meal. The co-formation of ye'elimite and alite is challenging due to their different thermal stability ranges, but if appropriate processing conditions and raw materials are used, an AYF cement clinker can be produced in a single stage at ~1250°C, which is approximately 200°C lower than that for conventional PC clinkers (Hanein et al., 2019).

The major drawback of AYF clinker manufacturing is the fact that clinkers with high sulfur content tend to have higher belite content (Herfort et al., 2010). S^{6+} and Al^{3+} can replace Si^{4+} in belite, which lowers the free energy of belite in a way that the combined free energy of belite and free lime is lower than that of alite, which prevents alite to form at low temperatures (Herfort et al., 2010). The incorporation of minor elements in belite and alite depends on their charge, size, and site occupancy (Tran et al., 2009; Herfort et al., 2010). Sulfur is incorporated in belite and alite as S^{6+}, which is small enough to replace Si^{4+} and has a strong preference for belite (Herfort et al., 2010). The maximum solubility of sulfur into belite as SO_3 is 2% (Herfort et al., 2010). The formation temperature of alite can be decreased through increasing its thermodynamic stability by lowering the free energy of alite at low temperatures. A mineralizer (F, Mg, Zn, or Cu) can be used to counteract the stabilization effect of sulfates on belite (Herfort et al., 2010). Moreover, fluoride has a strong mineralizing effect, especially with the coupled substitution of F^- for O^{2-} and Al^{3+} for Si^{4+} (Tran et al., 2009). Previous studies have already proven the concept of producing AYF cements using fluoride as a mineralizer (Blanco-Varela et al., 1995; Duvallet, 2014; Chitvoranund et al., 2017; Londono-Zuluaga et al., 2017; Hanein et al., 2019; Zea-Garcia et al., 2019, 2020). It has been confirmed that fluoride enhances the formation of alite phase in CaO-SiO₂-CaSO₄-CaF₂-Fe₂O₃ (Blanco-Varela et al., 1995; Duvallet, 2014; Londono-Zuluaga et al., 2017; Hanein et al., 2019; Zea-Garcia et al., 2019), CaO-SiO₂-CaF₂-CaSO₄ (Giminez-Molina et al., 1992), CaO-SiO₂-Al₂O₃-CaF₂-CaSO₄ (Giminez-Molina et al., 1992; Giménez-Molina and Blanco-Varela, 1995), and SiO₂-CaO-Al₂O₃-CaF₂ systems (Shame and Glasser, 1987). In the presence of fluoride, higher

[1]The cement oxide chemistry notation used in this work: C = CaO, S = SiO₂, A = Al₂O₃, F = Fe₂O₃, and $ = SO₃

FIGURE 1 | Effect of fluoride on the CaO-SiO₂–Al₂O₃-F system, where alite = Ca₃Si₁₋ₓAlₓO₅₋ₓFₓ and 0 > X > 0.3. Modified from Shame and Glasser (1987).

C_3S formation yields are achieved because phase formation energy is decreased (Pajares et al., 2002). Also, $CaSO_4$ and CaF_2 in the raw mix leads to liquid formation that enhances the ion mobility, which is referred to as a fluxing effect (Giminez-Molina et al., 1992; Giménez-Molina and Blanco-Varela, 1995). It has also been discussed that alumina (Shame and Glasser, 1987) (coupled substitution) and iron (Hanein et al., 2019) (effective firing efficiency) have a positive effect on the formation of the alite phase at lower temperatures.

Shame and Glasser (1987) have showed that Al and F can stabilize a solid solution of rhombohedral alite with a composition of $Ca_3Si_{1-x}Al_xO_{5-x}F_x$ in which the maximum substitution of fluoride was X = 0.15 (see **Figure 1**). With the addition of fluoride, the minimum formation temperature of the alite solid solution decreases from 1250°C (X = 0) to 1050°C (X = 0.15). When producing a AYF clinker, SO_3 is also present, which can also lead to the formation of fluorellestadite ($Ca_{10}(SiO_4)_3(SO_4)_3F_2$) (Pajares et al., 2002), which is reported to decompose at around 1250°C into C_2S, SO_2, O_2, and a liquid phase (Giminez-Molina et al., 1992; Blanco-Varela et al., 1995; Giménez-Molina and Blanco-Varela, 1995; Londono-Zuluaga et al., 2017; Hanein et al., 2019). Fluorellestadite has poor hydraulic characteristics and therefore is usually avoided in

TABLE 1 | List of reagent-grade chemicals used for clinker synthesis.

Chemical		CAS number	Supplier
Aluminum oxide (metals basis), fine powder	Al_2O_3	1344-28-1	Alfa Aesar
Calcium fluoride	CaF_2	7789-75-5	Fisher Scientific
Calcium oxide, reagent-grade powder	CaO	1305-78-8	Alfa Aesar
Calcium sulfate, anhydrous powder	$CaSO_4$	7778-18-1	Alfa Aesar
Iron (III) oxide (metals basis)	Fe_2O_3	1309-37-1	Alfa Aesar
Silicon oxide (trace metals basis)	SiO_2	60676-86-0	Sigma-Aldrich

clinker production (ben Haha et al., 2019). Additionally, under normal processing conditions, ye'elimite decomposes at temperatures above 1300°C (Hanein et al., 2015; Hanein, 2016); therefore, the ideal firing temperature in a standard fossil fuel combustion atmosphere or air for the production of a ye'elimite-rich clinker should be 1250–1300°C.

Iron is important for the burnability of the clinker, and it is known to improve the phase formation of calcium sulfoaluminate (CSA) clinkers, that is, fewer unreacted raw materials persist. However, the addition of iron can lead to the decomposition of ye'elimite, as a loss of SO_2 already occurs at lower processing temperatures (Puertas et al., 1995; el Khessaimi et al., 2018; Bullerjahn et al., 2020; Yao et al., 2020). It is also reported that the iron content enhances the formation of alite at lower temperatures (Chabayashi et al., 2012; Lu et al., 2018; Hanein et al., 2019).

Mayenite is a typical minor phase in alite–ye'elimite clinkers (Londono-Zuluaga et al., 2017; Zea-Garcia et al., 2019). The mayenite group has a common formula of $Ca_{12}Al_{14}O_{32-x}$ $(OH)_{3x}$ $[W_{6-3x}]$, where X = 0–2, and W can be occupied with anions OH^-, F^-, and Cl^- or H_2O (Środek et al., 2018) In tetrahedral sites, Al^{3+} can be replaced with, for example, Fe^{3+} and Si^{4+} (Galuskin et al., 2015; Środek et al., 2018). Synthetic crystalline mayenite has the structure $Ca_{12}Al_{14}O_{32}$, but, as was shown in common formula, the presence of F^- can lead to the stabilization of mayenite (Zhmoidin and Chatterjee, 1984; ben Haha et al., 2019) or the formation of fluormayenite $Ca_{12}Al_{14}O_{32}F_2$ (Galuskin et al., 2015; Środek et al., 2018).

(Hanein et al., 2019) prepared two relevant AYF clinkers with stoichiometric target compositions of C_3S-C_4A_3\$ and C_3S-C_4A_3\$-C_4AF with and without a fluoride addition at 1250°C. In their studies, they found that, with the fluoride addition to the C_3S-C_4A_3\$ clinker, the alite content increased from 0 to 12 wt%, and, when iron was present in the C_3S-C_4A_3\$-C_4AF clinker, the alite content doubled to around 24 wt%. This indicates that iron also plays a role in enhancing alite formation. Duvallet et al. (2009), Duvallet (2014), and Chitvoranund et al. (2017) prepared a clinker with 50 wt% C_3S and 10 wt% C_4A_3\$ at 1300 °C using 1 wt% calcium fluoride (CaF_2). They concluded that, with a 5 wt% anhydrite addition to the clinker, rapid hydration could be achieved, and the hydration products were calcium–silicate–hydrates (C–S–H), ettringite, monosulfate, and portlandite. In the studies of Duvallet et al. (2009) and Duvallet (2014), It was found that, with AYF clinkers produced at 1250–1275°C with 5 wt% to 45 wt% of ferrite using industrial by-products and virgin raw materials, including CaF_2, alite can be formed, but the hydration is reduced with an increasing ferrite content.

There is limited information in the literature regarding the optimal formation conditions of a clinker containing alite, ye'elimite, and ferrite as the major phases. Particularly, the sensitivity of fluctuations in the fluoride and iron content of the raw material mix is not fully understood. In the present study, 24 AYF cement clinkers were produced at 1250°C in three test series. In the first series, a target of 50 wt% C_3S, 30 wt% C_4A_3\$, and 20 wt% C_4AF was tested with seven compositions of fluoride (0 < x < 0.3 in $Ca_3Si_{1-x}Al_xO_{5-x}F_x$). For the second series, 50 wt% C_3S, 32.5–50 wt% C_4A_3\$, and 0–17.5 wt% C_4AF with fixed fluoride contents were assessed. In the third series, a phase composition of 28 wt% C_4A_3\$, 28–66 wt% C_3S, 0–37 wt% C_4AF, and 6 wt% C\$ with fixed fluoride content was targeted. The changes in the phase composition were examined based on the intensity of the reflection peaks in the XRD (X-ray diffraction) patterns, and the trend of the phase content was further analyzed using Rietveld analysis.

MATERIALS AND METHODS

The reagent-grade chemicals used were aluminum oxide, calcium fluoride, calcium oxide, calcium sulfate, iron (III) oxide, and silicon dioxide, as shown in **Table 1**. All reagent-grade chemicals—except CaF_2—were dried in a 500°C muffle furnace for 12 h. The chemical compositions for all three test series were calculated using the equations in **Table 2**. The target-phase compositions and the starting chemical composition of each test series are presented in **Table 3**.

The first test series was to determine the effect of adding fluoride to the clinkering with fixed phase contents. The phase composition was selected to be 50 wt% C_3S, 30 wt% C_4A_3\$, and 20 wt% C_4AF, and the fluoride content was adjusted according to $Ca_3Si_{1-x}Al_xO_{5-x}F_x$ between 0 < X < 0.3. The second and third test series were used to determine how iron effects the alite formation; in these test series, the fluoride contents were set to 1.3 wt% CaF_2 in the raw mix. In the second test series, the target C_3S content was fixed to 50 wt%, and the F content was also fixed (X = 0.15); moreover, the target C_4A_3\$ content was between 32.5 and 50 wt %, and the C_4AF between 0 and 17.5 wt%. In the test series 3, the potential sulfur loss through fluorellestadite decomposition was compensated with additional $CaSO_4$. Specifically, 1.3 wt% of CaF_2 (0.64 wt% F) theoretically can form 17 wt% of fluorellestadite ($Ca_{10}(SiO_4)_3(SO_4)_3F_2$; $3C_2S*3C\$*CaF_2$). If this occurs, it can decompose during firing at 1250°C, leading to a sulfur loss of 4 wt% as SO_3. In the third test series, the clinkers had a target C_3S

TABLE 2 | Equations to calculate the target phase composition.

Equations[a]

$Al_2O_3 = [C_4A_3\$ (wt\%)/(C_4A_3\$ (g/mol)/3Al_2O_3 (g/mol)] + [C_4AF (wt\%) /(C_4AF (g/mol) /Al_2O_3 (g/mol)]$
$CaO = [C_4A_3\$ (wt\%)/(C_4A_3\$ (g/mol)/4CaO (g/mol)] + [C_4AF (wt\%) /(C_4AF (g/mol) /4 CaO(g/mol)] + [C_3S (g/mol) /(3 CaO (g/mol))]$
$Fe_2O_3 = [C_4AF (wt\%)/(C_4AF (g/mol) /Fe_2O_3 (g/mol))]$
$SiO_2 = [C_3S (wt\%)/(C_3S (g/mol)/SiO_2 (g/mol))]$
$SO_3 = [C_4A_3\$ (wt\%)/(C_4A_3\$ (g/mol)/SO_3 (g/mol))]$

[a]No corrections were made for possible elemental substitutions. In test series 3, extra $CaSO_4$ was added.

TABLE 3 | Target-phase compositions (wt%) and raw material mix chemical compositions of test series 1–3 (wt%).

Target compositions				Raw material mix compositions						
Series 1	C_3S	$C_4A_3\$$	C_4AF	C$	C	S	A	F	C$	CaF_2	Fluoride content as X in $(Ca_3Si_{1-x}Al_xO_{5-x}F_x)$
X = 0	50	30	20	0	54.36	13.16	19.23	6.57	6.68	0	0
X = 0.025	50	30	20	0	54.24	13.13	19.19	6.56	6.67	0.21	0.025
X = 0.0375	50	30	20	0	54.18	13.12	19.17	6.55	6.66	0.32	0.0375
X = 0.075	50	30	20	0	54.01	13.08	19.1	6.53	6.64	0.64	0.075
X = 0.15	50	30	20	0	53.66	12.99	18.98	6.49	6.6	1.29	0.15
X = 0.225	50	30	20	0	53.31	12.91	18.86	6.45	6.55	1.93	0.225
X = 0.3	50	30	20	0	52.95	12.82	18.73	6.4	6.51	2.58	0.3
Series 2											
0 C4AF	50	50	0	0	50	12.99	24.73	0	10.99	1.29	0.15
2.5 C4AF	50	47.5	2.5	0	50.45	12.99	24.01	0.81	10.44	1.29	0.15
5 C4AF	50	45	5	0	50.91	12.99	23.29	1.62	9.89	1.29	0.15
7.5 C4AF	50	42.5	7.5	0	51.37	12.99	22.57	2.43	9.35	1.29	0.15
10 C4AF	50	40	10	0	51.83	12.99	21.86	3.25	8.8	1.29	0.15
12.5 C4AF	50	37.5	12.5	0	52.28	12.99	21.14	4.06	8.25	1.29	0.15
15 C4AF	50	35	15	0	52.74	12.99	20.42	4.87	7.7	1.29	0.15
17.5 C4AF	50	32.5	17.5	0	53.2	12.99	19.7	5.68	7.15	1.29	0.15
Series 3											
0 C_4AF	66	28	0	6	53.89	17.45	14.23	0	13.11	1.32	0.11
5 C_4AF	61	28	5	6	52.59	16.2	15.23	1.56	13.11	1.32	0.12
10 C_4AF	56	28	9	6	51.29	14.95	16.22	3.11	13.11	1.32	0.13
15 C_4AF	52	28	14	6	49.98	13.71	17.21	4.67	13.11	1.32	0.14
20 C_4AF	47	28	19	6	48.68	12.46	18.21	6.22	13.11	1.32	0.16
25 C_4AF	42	28	23	6	47.38	11.21	19.2	7.78	13.11	1.32	0.18
30 C_4AF	37	28	28	6	46.07	9.97	20.19	9.34	13.11	1.32	0.20
35 C_4AF	33	28	33	6	44.77	8.72	21.19	10.89	13.11	1.32	0.23
40 C_4AF	28	28	37	6	43.46	7.48	22.18	12.45	13.11	1.32	0.27

First series with a target of 50 wt% C_3S, 30 wt% $C_4A_3\hat{S}$, and 20 wt% C_4AF with seven compositions of fluoride according to $Ca_3Si_{1-x}Al_xO_{5-x}F_x$, with 0 < X < 0.3; weighted values not normalized. Second series C_3S 50 wt%, $C_4A_3\hat{S}$ 32.5–50 wt%, and C_4AF 0–17.5 wt% with a fixed fluoride content of 1.29 wt% CaF_2; weighted values not normalized. Third series with target-phase compositions of 28 wt% $C_4A_3\hat{S}$, 28–66 wt% C_3S, 0–37 wt% C_4AF, and 6 wt% C$ with fixed fluoride content (1.32 wt% CaF_2); values normalized to 100%. Some additional Ca is present because fluoride was added as CaF_2.

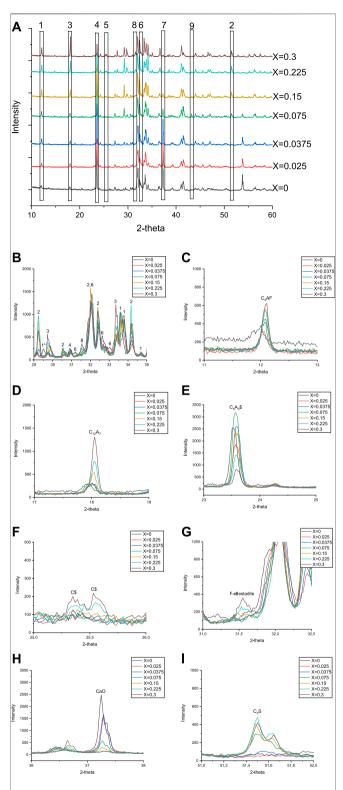of 28–66 wt% and a target C_4AF of 0–37 wt%, and the SO_3 was kept constant with a target $C_4A_3\$$ of 28 wt% and C$ of 6 wt%.

CLINKERING PROCEDURE

To prepare the clinker batches, 25 g of each combination (see **Table 3**) were manually ground for ~20 min using a mortar and pestle to obtain a homogenous mixture. From the mixtures, 5 g was weighed in 20 ml alumina crucibles and placed into a muffle furnace preheated to 800°C; then, a 30-min hold was applied, followed by heating with a ramp of 5°C/min to 1250°C, at which

the temperature was held for 90 min. After thermal treatment, the samples were removed from the furnace (at a clinkering temperature of 1250°C) and then allowed to quench in the air at room temperature. The cooled clinkers were ground by hand with an agate mortar and pestle to fine powders for XRD analysis.

MATERIAL CHARACTERIZATION

The diffractograms for each clinker were obtained using X-ray diffraction (Bruker D2 PHASER: Cu Kα1, λ = 1.54184 Å). The parameters of the XRD analysis were a 2θ range of 10–70°, a Cu
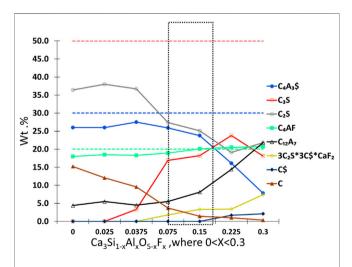
FIGURE 2 | XRD diffractograms of series 1 with phase identification **(A)**. Magnified sections of interest from 2-theta 29–35° **(B)**. 1. C_4AF, 1*C_4AF (alumina rich), 2. C_3S, 3. $C_{12}A_7$, 4. $C_4A_3\$$, 5. C$, 6. C_2S, 7. CaO, 8. fluorellestadite, and 9. Al_2O_3. CaO = unreacted lime, C_3S = alite, $C_{12}A_7$ = mayenite, $C_4A_3\$$ = ye'elimite, C_4AF = brownmillerite, and F-ellestadite = fluorellestadite. Magnified sections of single phases are presented in **C–I**.

Kα radiation of 30 V and 10 mA, and a step size of 0.02° with 0.4 s per step. The samples were back-loaded using PW1811 sample holders. During the XRD scan, the sample was rotated at 15 rpm, and a 1-mm divergence splitter was used while the Ni-K filter was removed. The lower discriminator was set to 0.19, and the upper discriminator to 0.28. First, the phases were identified from diffraction patterns using EVA software (Bruker), and further Rietveld analysis was done using PDXL 2 (Rigaku) software with the PDF-4+ 2020 RDB database to determine the changes in the phase trend in the samples. The preferred crystallographic information for the phase identification included C_4AF (Redhammer et al., 2004), C_3S (Mumme, 1995), $C_{12}A_7$ (Palacios et al., 2008), $C_4A_3\$$ (Cuesta et al., 2013), C$ (Morikawa et al., 1975), C_2S (Mumme et al., 1995), CaO (Smith and Leider, 1968), fluorellestadite (Pajares et al., 2002), and Al_2O_3 (Lewis et al., 1982)(ben Haha et al., 2019).
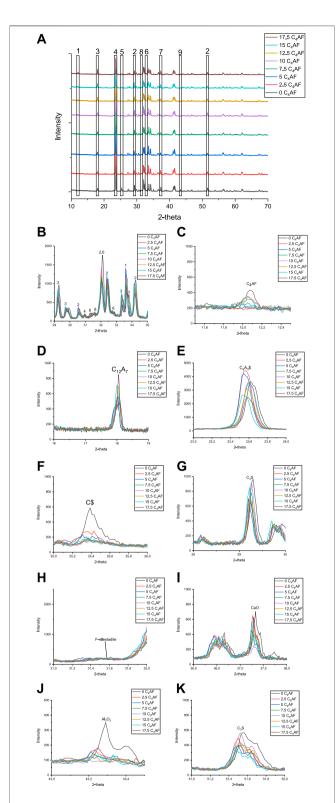
RESULTS

The results comparing the intensity of the diffraction patterns are shown in **Figures 2**, **4**, and **6**. The phase composition trend is shown in **Figures 3**, **5**, and **7**. The Rietveld analysis and error (difference between the target and back-calculated chemical composition from the Rietveld analysis) data of series 1–3 are shown in the appendix (**Supplementary Appendix Table A1, A2**).

Series 1: Effect of Varying Fluoride (X) Content in $Ca_3Si_{1-x}Al_xO_{5-x}F_x$

In this series, the effect of different amounts of fluoride in the raw mix was tested. The target clinker composition was 50 wt% C_3S,

FIGURE 3 | Target-phase composition (dashed lines) and the trend in the phase contents in the first test series acquired from the Rietveld analysis. The optimal phase content zone is marked with a dotted marker box. C_4AF = ferrite, C_3S = alite, $C_{12}A_7$ = mayenite, $C_4A_3\$$ = ye'elimite, C$ = anhydrite, C_2S = larnite, CaO = free lime, Al_2O_3 = free alumina, and $3C_2S*3C\$*CaF_2$ = fluorellestadite.
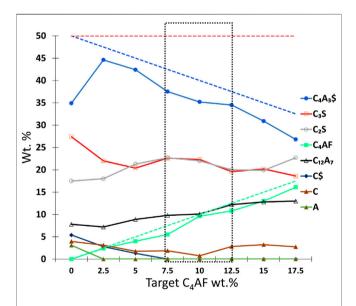
FIGURE 4 | XRD diffractograms of series 2: Magnified sections of interest from 2-theta 29–35°. 1. C_4AF, 2. C_3S, 3. $C_{12}A_7$, 4. $C_4A_3\$$, 5. C$, 6. C_2S, 7. CaO, 8. fluorellestadite, and 9. Al_2O_3. CaO = unreacted lime, C_3S = alite, $C_{12}A_7$ = mayenite, $C_4A_3\$$ = ye'elimite, C_4AF = brownmillerite, and F-ellestadite = fluorellestadite. Magnified sections of single phases are presented in **Figure 4C-K**.
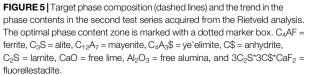
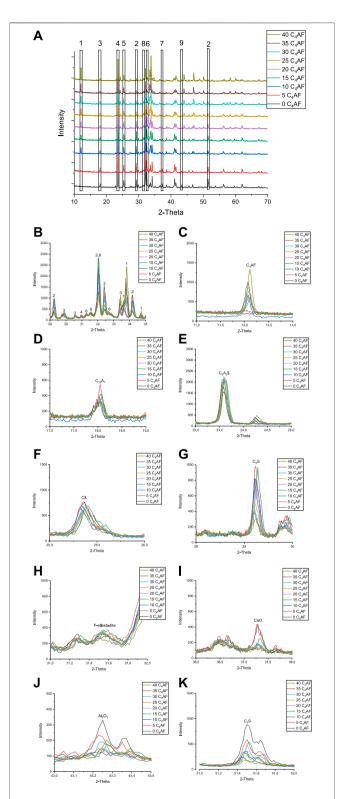30 wt% $C_4A_3\$$, and 20 wt% C_4AF. An overview of the XRD diffractograms is presented in **Figure 2**.

In **Figure 2D** with X > 0.15, the peak of mayenite (18.05°) increases with the decrease in ye'elimite (peak at 23.56°) instead that is shown in **Figure 2E**. Fluorellestadite (31.53°) clearly appears when fluoride content increases to X > 0.15 (**Figure 2G**). With low amounts of fluoride in clinker, there was unreacted lime, which can be seen as intensity peaks at 2-theta 37.25° and 53.77° (see **Figure 2H**). Alite content was close to zero in low fluoride-containing samples (see **Figure 2I**). From the fluoride content of X = 0.075 upward, the amount of unreacted lime starts to decrease and the peak of alite appears at 51.5° and grows up to X = 0.225 (**Figure 2I**). An increase in fluoride content leads to liquid formation during firing. More liquid during firing allows more brownmillerite (peak at 12.09°) to crystallize (ben Haha et al., 2019). The highest fluoride content led to the highest content of mayenite, fluorellestadite, and anhydrite together with the lowest content of ye'elimite. The trend of phase compositions of first test series is presented in **Figure 3**. The trend shows that target phases C_3S, $C_4A_3\$$, and C_4AF are achieved in adequate levels when the fluoride content is around X = 0.15, and thereby the fluoride content was selected also for test series 2.

Series 2: Effect of Target Ferrite/Ye'elimite Ratio in AYF

Based on the results of test series 1, the fluoride content in series 2 was fixed to X = 0.15. In this series, the silica and fluoride content was kept constant (CaF_2 = 1.29 wt%). The target phase compositions were C_3S 50 wt%, $C_4A_3\$$ 32.5–50 wt%, and C_4AF 0–17.5 wt%. The

FIGURE 5 | Target phase composition (dashed lines) and the trend in the phase contents in the second test series acquired from the Rietveld analysis. The optimal phase content zone is marked with a dotted marker box. C_4AF = ferrite, C_3S = alite, $C_{12}A_7$ = mayenite, $C_4A_3\$$ = ye'elimite, C$ = anhydrite, C_2S = larnite, CaO = free lime, Al_2O_3 = free alumina, and $3C_2S*3C\$*CaF_2$ = fluorellestadite.
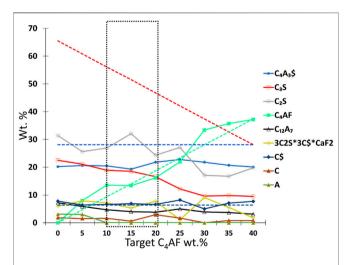
FIGURE 6 | XRD-diffractograms of series 3 with phase identification (**Figure 6A**). Magnified sections of interest from 2-theta 29–35°. (**Figure 6B**). 1. C_4AF, 2. C_3S, 3. $C_{12}A_7$, 4. $C_4A_3\$$, 5. $C\$$, 6. C_2S, 7. CaO, 8. fluorellestadite, and 9. Al_2O_3. CaO = unreacted lime, C_3S = alite, $C_{12}A_7$ = mayenite, $C_4A_3\$$ = ye'elimite, C_4AF = brownmillerite, and F-ellestadite = fluorellestadite. Magnified sections of single phases are presented in **Figure 6C-K**.

diffractograms (**Figure 4A**), as well as the magnified sections from (**Figure 4B–K**) the diffractogram, are shown.

In **Figure 4**, the sample 0 C_4AF (50–50 $C_4A_3\$$-C_3S) has a clear peak of alite (at 51.5°) that indicates fluoride alone can stabilize alite; however, the presence of unreacted CaO (**Figure 4I**) and Al_2O_3 (**Figure 4J**) indicate that iron is required to enhance the burnability at 1250°C, and only a small amount of iron content in the mix was required. Moreover, Al_2O_3 disappears in the sample with a target of 2.5 wt% C_4AF, and the peak of $C\$$ completely disappears in the sample with a target of 7.5 wt% C_4AF. The increase in iron content and decrease in sulfur content in the raw mix led to an increase in the mayenite/ye'elimite ratio. With the fixed fluoride content (X = 0.15), there was no fluorellestadite present in any samples. The trend in the phase composition of the second test series is presented in **Figure 5**. The free lime content was the lowest in 10 C_4AF, with a mayenite/ye'elimite ratio at an adequate level, when compared to target. However, the amount of produced alite in the 7.5 C_4AF, 10 C_4AF, and 12.5 C_4AF samples was only around 45% of the target; the amount of alite in these samples was the highest of all the samples with iron.

Series 3: Effect of Target Ferrite/Alite Ratio in AYF

In test series 3, the sulfur contents in the raw material mixtures were kept constant, although alite content was changing. The sulfur content in raw mix was double when compared to test series 1 and 2 to see if extra sulfur has an effect on phase formation. The target phase compositions were 28 wt% of $C_4A_3\$$, 28–66 wt% of C_3S, 0–37 wt% of C_4AF, and 6 wt% $C\$$. In the test series 1 and 2, fluoride content was proportional to the alite content. In test series 3, the proportion of fluoride in alite is

FIGURE 7 | Target-phase composition (dashed lines) and the phase content trend in the third test series was obtained from the Rietveld analysis. The optimal phase content zone is marked with a dotted marker box. C_4AF = ferrite, C_3S = alite, $C_{12}A_7$ = mayenite, $C_4A_3\$$ = ye'elimite, $C\$$ = anhydrite, C_2S = larnite, CaO = free lime, Al_2O_3 = free alumina, and $3C_2S*3C\$*CaF_2$ = fluorellestadite.

TABLE 4 | Fluoride content according to alite content.

Sample	Alite C$_3$S (wt%)	X, Ca$_3$Si$_{1-x}$Al$_x$O$_{5-x}$F$_x$
0 C$_4$AF	66	0.11
5 C$_4$AF	61	0.12
10 C$_4$AF	56	0.13
15 C$_4$AF	52	0.14
20 C$_4$AF	47	0.16
25 C$_4$AF	42	0.18
30 C$_4$AF	37	0.20
35 C$_4$AF	33	0.23
40 C$_4$AF	28	0.27

changing as presented in **Table 4**. The XRD diffractograms are presented in **Figure 6**.

As highlighted in the magnified sections in **Figure 6**, both mayenite (**Figure 6D**) and anhydrite (**Figure 6F**) were observed in all samples. Also, as in series 2, the samples with a low iron content, 0 C$_4$AF, and 5 C$_4$AF had unreacted CaO (**Figure 6I**) and Al$_2$O$_3$ (**Figure 6J**). When C$_4$AF in the target composition increases, the content of unreacted CaO and Al$_2$O$_3$ reduces, and C$_4$AF peaks are observable at 12.1°. As shown in series 1 and 2, iron content has an impact on the burnability of the constituents of the mixes. It is necessary to inhibit the persistence of uncombined CaO and other raw materials but only up to a certain extent, and a ferrite content of >10 wt% is not necessary for a complete reaction.

Unlike in series 1, ye'elimite content in series 3 remains constant in all the raw mixes. In series 1, the increasing fluoride content led to less ye'elimite. It seems that here in series 3, with constant fluoride (1.32 wt%) content in the raw mix, the ye'elimite also remains stable. Excess anhydrite remains unreacted that indicate excess sulfur is not the dominating factor to prevent decomposition of ye'elimite. The amount of belite is not increasing when compared to other test series that can be explained with maximum solubility of sulfur into belite (2% as SO$_3$) (Herfort et al., 2010).

ADDITIONAL DISCUSSION

In test series 1–3, it is shown that fluoride provides a sufficient driving force to the alite formation at 1250°C—even though sulfur is present. It was shown in series 2 and 3 that alite can form when fluoride and alumina are present without iron, as also shown by Shame and Glasser (1987). As discussed in the introduction section, sulfur tends to stabilize belite, and, therefore, a mineralizer (fluoride) must be added to prevent belite formation to achieve alite formation. The percentage of alite formed compared to the target composition is presented in **Table 5**. It is shown that the alite content in the produced clinkers in series 2 and 3 when compared to the target composition was between 28 and 55 wt%. Further investigation and thermodynamic understanding of the system is necessary in order to design/formulate AYF clinkers.

It is known that iron can substitute for ye'elimite (Bullerjahn et al., 2020) and mayenite (Ruttanapun et al.,

2018) as well as vary the alumina/iron ratio in the ferrite phase (Redhammer et al., 2004). Rigorous microstructural characterization was not the aim of this study, and the chemical substitution was not tested in the title study. The substitution of iron and fluoride should be further studied using spectroscopic techniques. Also, iron can substitute for alite and belite in small amounts. Results from series 2 suggest that fluoride can be assumed to substitute for alite phase and/or mayenite (fluormayenite) (Środek et al., 2018) since no fluorellestadite was formed. It is known that F does not substitute for belite, which is the key factor in fluoride working as a mineralizer for alite (Herfort et al., 2010; Hewlett et al., 2019).

As shown in the results, mayenite was formed in all clinkers and fluorellestadite in test series 1 and 3. Mayenite was present in all samples regardless of the amount of fluoride added. It has been found that, in CSA clinkers, a fast cooling rate can lead to mayenite formation, which could explain the formation of mayenite even without the presence of fluoride (x = 0, series 1) (Dolenec et al., 2020). Another explanation might be the substitution of Fe or Si with Al, but this is out of the scope of the title study. Mayenite and fluorellestadite formation is not optimal for clinker hydration properties due to poor hydraulic characteristics. Moreover, it has been discussed that fluorellestadite has poor hydraulic characteristics (ben Haha et al., 2019) and should be avoided in clinkers, especially since it consumes valuable oxides from raw materials that could form more hydraulic phases. Mayenite is usually unfavorable because of its very fast hydration speed. The faster hydration speed of mayenite compared to ye'elimite is explained with its higher Ca/Al ratio (Hewlett et al., 2019; Bullerjahn et al., 2020). The formation of mayenite is not as disadvantageous in terms of hydration as the formation of fluorellestadite because it hydrates to form ettringite or monosulfate (Nguyen et al., 2019) and the hydration of mayenite can be controlled with the addition of retarders (Gijbels et al., 2019). Retarders, such as citric acid, have been proven to work in CSA cements (Moir, 1983; Gijbels et al., 2019), PC–CSA-C$ mix (Pelletier et al., 2010), and mayenite-rich ladle slag–phosphogypsum mix (Nguyen et al., 2019). Also, the presence of fluoride might produce a positive effect on the workability of the cement by retarding the fast-reacting clinker. Fluoride is known to have a retarding effect in CSA mixes (Jun et al., 2001; Liu et al., 2016) and in mayenite-rich ladle slag–phosphogypsum mix (Gijbels et al., 2019). Further, in PC, it is shown that fluoride first increases the hydration speed but has a retarding effect after a certain threshold (0.37 wt% fluoride in bulk composition) (Moir, 1983; Tran, 2011). The presence of fluoride slows down the hydration, but, with longer hydration times, the compressive strength reaches the same or a higher level as fluoride-free cement after complete hydration (Tran, 2011; Hanein et al., 2018; Gálvez-Martos et al., 2020).

In series 1, both the fluorellestadite and mayenite content increased with the higher fluoride content of the clinker. It was seen that with an adequate fluoride content (X = 0.075–0.15), ye'elimite can coexist with alite and form a clinker with a high

TABLE 5 | Target alite content compared to alite content from the Rietveld analysis.

Sample	Alite Rietveld (wt%)	Alite target (wt%)	Rietveld/target (%)
		Series 1	
X = 0	0	50	0
X = 0.025	0	50	0
X = 0.0375	3	50	7
X = 0.075	17	50	34
X = 0.15	18	50	36
X = 0.225	24	50	48
X = 0.3	18	50	36
		Series 2	
0 C_4AF	27	50	55
2.5 C_4AF	22	50	44
5 C_4AF	20	50	41
7.5 C_4AF	23	50	45
10 C_4AF	22	50	45
12.5 C_4AF	20	50	39
15 C_4AF	20	50	40
17.5 C_4AF	19	50	37
		Series 3	
0 C_4AF	23	65	35
5 C_4AF	21	61	35
10 C_4AF	19	56	34
15 C_4AF	19	51	37
20 C_4AF	17	47	36
25 C_4AF	12	42	28
30 C_4AF	10	37	27
35 C_4AF	10	33	31
40 C_4AF	10	28	36

hydraulic cement-phase content. The SO_3 and fluoride content in the clinker raw mix seems to have a significant effect on the interactions between the mayenite–ye'elimite and fluorellestadite phases. In series 2, with an adequate $CaSO_4$ content for stoichiometric ye'elimite formation, fluorellestadite was not formed, but the mayenite content increased with the increasing iron content. In series 3, with the additional $CaSO_4$ introduced to the raw mix, fluorellestadite was present in increased amounts, but the mayenite and ye'elimite content were constant. The conclusions from series 2 and 3 were that the SO_3 content in the clinker mix needs to be optimized in a way that there is sufficient SO_3 in the ye'elimite formation to prevent mayenite formation—but not in a large excess that enables undesirable fluorellestadite formation/persistence in the final clinker.
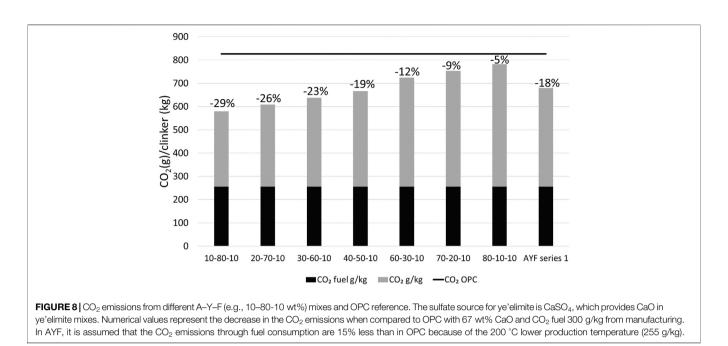
BRIEF SUSTAINABILITY PERFORMANCE ASSESSMENT

The effect of a raw mix design on the CO_2 emissions of the AYF clinker compared to PC clinker is shown in **Figure 8**. It is shown that with the mix introduced in series 1, the CO_2 emissions combined from the fuel consumption of the manufacturing and $CaCO_3$ required for the raw mix are 18% less than with OPC; however, the total CO_2 emissions also depend on other factors, and, in particular, emissions from obtaining the raw materials can have a large influence on

CO_2 emissions, especially if travelling long distances, as shown, for example, in the location of the bauxite source for the production of ye'elimite-rich cement (Hanein et al., 2018; Gálvez-Martos et al., 2020). It was noted in this study that increasing iron and fluoride contents made the clinkers more difficult to grind, which might cause extra manufacturing costs.

The fluoride required for AYF clinker production can be provided using industrial waste materials, such as argon oxygen decarburization (AOD) slags or aluminum salt slags for use as clinker raw materials. These side streams also contain significant quantities of CaO, Al_2O_3, SiO_2, and Fe_2O_3 which are crucial for clinker production but usually avoided because of the presence of fluoride; however, this work suggests that these can be repurposed for use in AYF clinker manufacturing.

CONCLUSION

The target AYF composition was not achieved in any of the clinkers as the formation/persistence of belite and mayenite could not be avoided in the presence of sulfur, the belite phase is forming and appears to consume SiO_2 and CaO that were targeted for the alite formation. Minor phase mayenite was present, and its formation was increased with the fluoride content.

FIGURE 8 | CO_2 emissions from different A–Y–F (e.g., 10–80–10 wt%) mixes and OPC reference. The sulfate source for ye'elimite is $CaSO_4$, which provides CaO in ye'elimite mixes. Numerical values represent the decrease in the CO_2 emissions when compared to OPC with 67 wt% CaO and CO_2 fuel 300 g/kg from manufacturing. In AYF, it is assumed that the CO_2 emissions through fuel consumption are 15% less than in OPC because of the 200 °C lower production temperature (255 g/kg).

The optimal fluoride content for the clinker was achieved with a target composition of 50 wt% C_3S, 30 wt% $C_4A_3\$$, and 20 wt% C_4AF with fluoride content between $0.075 \leq X \leq 0.15$ in $Ca_3Si_{1-x}Al_xO_{5-x}F_x$. Fluoride has an important effect on the formation of alite when the clinker is produced at 1250°C but can lead to the formation of fluorellestadite when excess sulfur is present in the clinker raw mix. A slight addition of fluoride ($X = 0.075$) leads to the desired alite formation, but too much fluoride content reduces the ye'elimite content and leads to the formation of undesirable mayenite, fluorellestadite, and unreacted raw materials (anhydrite, CaO, or alumina). All clinkers with a fluoride content between $x = 0.075$ and $x = 0.1$ in $Ca_3Si_{1-x}Al_xO_{5-x}F_x$ had alite in their products. In series 3, almost all the excess anhydrite remained unreacted and did not further stabilize belite over alite. The effect of extra SO_3 on stabilization needs to be further studied.

Fe_2O_3 is crucial to the burnability of AYF clinkers, but only to a certain extent. It was shown that 10 wt% C_4AF as the target composition is sufficient to avoid unreacted raw materials. The effect of the amount of Fe_2O_3 and Al_2O_3 in the AYF system needs to be studied in further experiments, especially as the Fe content can be incorporated in both the ye'elimite and mayenite structures. Due to the complexity of the interactions in such clinkering systems, thermodynamic assessment and modeling will be crucial in their design.

The outcomes of this work improve understanding of low-carbon AYF cement clinker raw mix design and can promote waste valorization and circularization by enabling the use of fluoride-containing waste in cement clinker manufacturing.

DATA AVAILABILITY STATEMENT

The raw data supporting the conclusion of this article will be made available by the authors, upon reasonable request.

AUTHOR CONTRIBUTIONS

VI: first author, conceptualization, methodology, validation, formal analysis, investigation, visualization, writing (original draft), and writing (review and editing). KO: conceptualization and writing (review and editing). TH and HK: conceptualization, methodology, validation, and writing (review and editing). PT: conceptualization, writing (review and editing), funding acquisition, and project administration. MI: conceptualization and writing (review and editing). TF: corresponding author, conceptualization, writing (review and editing), funding acquisition, and project administration. All authors contributed to the article and approved the submitted version.

FUNDING

ACKNOWLEDGMENTS

SUPPLEMENTARY MATERIAL

The Supplementary Material for this article can be found online at: https://www.frontiersin.org/articles/10.3389/fbuil.2021.698830/full#supplementary-material

REFERENCES

Barcelo, L., Kline, J., Walenta, G., and Gartner, E. (2014). Cement and Carbon Emissions. *Mater. Struct.* 47, 1055–1065. doi:10.1617/s11527-013-0114-5

ben Haha, M., Winnefeld, F., and Pisch, A. (2019). Advances in Understanding Ye'elimite-Rich Cements. *Cement Concrete Res.* 123, 105778. doi:10.1016/j.cemconres.2019.105778

Blanco-Varela, M. T., Palomo, A., Puertas, F., and Vázquez, T. (1995). Influencia de la incorporación conjunta del CaF2 y del CaSO4 en el proceso de clinkerización. Obtención de nuevos cementos. *Mater. Construcc.* 45, 21–39. doi:10.3989/mc.1995.v45.i239.551

Bullerjahn, F., Scholten, T., Scrivener, K. L., ben Haha, M., and Wolter, A. (2020). Formation, Composition and Stability of Ye'elimite and Iron-Bearing Solid Solutions. *Cement Concrete Res.* 131, 106009. doi:10.1016/j.cemconres.2020.106009

Cembureau (2019). *The European Cement Association, Activity Report 2018, Brussels.* Available at: https://cembureau.eu/media/clkdda45/activity-report-2019.pdf (Accessed February 25, 2021)

Chabayashi, T., Nagata, H., Nakamura, A., and Kato, H. (2012). Reduction of Burning Temperature of Cement Clinker by Adjusting of mineral Composition. *Cement Sci. Concrete Technology.* 66, 217–222. doi:10.14250/cement.66.217

Chitvoranund, N., Winnefeld, F., Hargis, C. W., Sinthupinyo, S., and Lothenbach, B. (2017). Synthesis and Hydration of Alite-Calcium Sulfoaluminate Cement. *Adv. Cement Res.* 29, 101–111. doi:10.1680/jadcr.16.00071

Cuesta, A., de La Torre, A. G., Losilla, E. R., Peterson, V. K., Rejmak, P., Ayuela, A., et al. (2013). Structure, Atomistic Simulations, and Phase Transition of Stoichiometric Yeelimite. *Chem. Mater.* 25, 1680–1687. doi:10.1021/cm400129z

Dolenec, S., Šter, K., Borštnar, M., Nagode, K., Ipavec, A., and Žibret, L. (2020). Effect of the Cooling Regime on the Mineralogy and Reactivity of Belite-Sulfoaluminate Clinkers. *Minerals.* 10, 910. doi:10.3390/min10100910

Duvallet, T., Henke, K., and Jewell, R. B. (2009). "Low-Energy, Low CO2-Emitting Cements Produced from Coal Combustion By-Products and Red Mud GHG Emissions from Uncontrolled Coal Fires," in World of Coal Ash (WOCA). Conference (Lexington, KY, USA. doi:10.13140/2.1.1538.2404

Duvallet, T. Y. (2014). Influence of Ferrite Phase in Alite-Calcium Sulfoaluminate Cements. Theses Dissertations. *Chemical Mater. Eng.* Available at: https://uknowledge.uky.edu/cme_etds/27 (Accessed February 25, 2021)

el Khessaimi, Y., el Hafiane, Y., Smith, A., Trauchessec, R., Diliberto, C., and Lecomte, A. (2018). Solid-state Synthesis of Pure Ye'elimite. *J. Eur. Ceram. Soc.* 38, 3401–3411. doi:10.1016/j.jeurceramsoc.2018.03.018

Galuskin, E. v., Gfeller, F., Galuskina, I. O., Armbruster, T., Bailau, R., and Sharygin, V. v. (2015). Mayenite Supergroup, Part I: Recommended Nomenclature. *Eur. J. Mineral.* 27, 99–111. doi:10.1127/ejm/2015/0027-2418

Gálvez-Martos, J., Valente, A., Martínez-Fernández, M., and Dufour, J. (2020). Eco-efficiency Assessment of Calcium Sulfoaluminate Clinker Production. *J. Ind. Ecol.* 24, 695–706. doi:10.1111/jiec.12967

Gartner, E. (2004). Industrially Interesting Approaches to "low-CO2" Cements. *Cement Concrete Res.* 34, 1489–1498. doi:10.1016/j.cemconres.2004.01.021

Gijbels, K., Nguyen, H., Kinnunen, P., Schroeyers, W., Pontikes, Y., Schreurs, S., et al. (2019). Feasibility of Incorporating Phosphogypsum in Ettringite-Based Binder from Ladle Slag. *J. Clean. Prod.* 237, 117793. doi:10.1016/j.jclepro.2019.117793

Giménez-Molina, S., and Blanco-Varela, M. T. (1995). Solid State Phases Relationship in the CaOSiO2Al2O3CaF2CaSO4 System. *Cement Concrete Res.* 25, 870–882. doi:10.1016/0008-8846(95)00078-Q

Giminez-Molina, S., Blanco, M. T., Marr, J., and Glasser, F. P. (1992). Phase Relations in the System Ca2SiO4-CaO-CaSO4-CaF2relevant to Cement Clinkering. *Adv. Cement Res.* 4, 81–86. doi:10.1680/adcr.1992.4.14.81

Hanein, T. (2016). *Development of a Novel Calcium Sulfoaluminate Cement Production Process.* Available at: https://abdn.alma.exlibrisgroup.com/view/delivery/44ABE_INST/12153080390005941 (Accessed February 25, 2021)

Hanein, T., Duvallet, T. Y., Jewell, R. B., Oberlink, A. E., Robl, T. L., Zhou, Y., et al. (2019). Alite Calcium Sulfoaluminate Cement: Chemistry and Thermodynamics. *Adv. Cement Res.* 31, 94–105. doi:10.1680/jadcr.18.00118

Hanein, T., Elhoweris, A., Galan, I., Glasser, F. P., and Bannerman, M. N. C. (2015). *Thermodynamic Data of Ye'elimite (C4A3$\overline{S}$) for Cement Clinker Equilibrium Calculations.* Available at: https://abdn.pure.elsevier.com/en/publications/thermodynamic-data-of-yeelimite-c4a3s-for-cement-clinker-equilibr (Accessed March 31, 2021)

Hanein, T., Galvez-Martos, J.-L., and Bannerman, M. N. (2018). Carbon Footprint of Calcium Sulfoaluminate Clinker Production. *J. Clean. Prod.* 172, 2278–2287. doi:10.1016/j.jclepro.2017.11.183

Hanein, T., Glasser, F. P., and Bannerman, M. N. (2020). Thermodynamic Data for Cement Clinkering. *Cement Concrete Res.* 132, 106043. doi:10.1016/j.cemconres.2020.106043

Herfort, D., Moir, G. K., Johansen, V., Sorrentino, F., and Arceo, H. B. (2010). The Chemistry of Portland Cement Clinker. *Adv. Cement Res.* 22, 187–194. doi:10.1680/adcr.2010.22.4.187

Hewlett, P., Liska, M., and Lea, F. M. (2019). *Lea's Chemistry of Cement and Concrete.* 5th ed. Oxford: Butterworth-Heinemann

Jun, C., Xin, C., Futian, L., Lingchao, L., and Bing, T. (2001). Influence of Fluorite on the Ba-Bearing Sulphoaluminate Cement. *Cement Concrete Res.* 31, 213–216. doi:10.1016/S0008-8846(00)00450-6

Lewis, J., Schwarzenbach, D., and Flack, H. D. (1982). Electric Field Gradients and Charge Density in Corundum, α-Al2O3. *Acta Cryst. Sect A.* 38, 733–739. doi:10.1107/S0567739482001478

Liu, B., Wang, S., Chen, Y., Gong, C., and Lu, L. (2016). Effect of Waste gypsum on the Setting and Early Mechanical Properties of belite-C2.75B1.25A3$ Cement. *J. Therm. Anal. Calorim.* 125, 75–83. doi:10.1007/s10973-016-5265-5

Londono-Zuluaga, D., Tobón, J. I., Aranda, M. A. G., Santacruz, I., and de la Torre, A. G. (2017). Clinkering and Hydration of Belite-Alite-Ye´elimite Cement. *Cement and Concrete Composites.* 80, 333–341. doi:10.1016/j.cemconcomp.2017.04.002

Lu, X., Li, C., Wang, S., Ye, Z., and Cheng, X. (2017). Effect of Ferrite Phase on the Formation and Coexistence of 3CaO.3Al₂O₃.CaSO₄ AND 3CaO.SiO₂ Minerals. *Ceramics - Silikaty.* 62, 67–73. doi:10.13168/cs.2017.0046

Moir, G. K. (1983). IMprovements in the Early Strength Properties of Portland Cement. *Trans. R. Soc, and A* 310 (1511), 127–138. doi:10.1098/rsta.1983.0072

Morikawa, H., Minato, I., Tomita, T., and Iwai, S. (1975). Anhydrite: a Refinement. *Acta Crystallogr. Sect B.* 31, 2164–2165. doi:10.1107/s0567740875007145

Mumme, W. G. (1995). Crystal Structure of Tricalcium Silicate from a Portland Cement Clinker and its Application to Quantitative XRD Analysis. *Neues Jahrbuch Für Mineralogie-Monatshefte* 4, 146–160.

Mumme, W. G., Hill, R. J., Bushnell-Wye, G., and Segnit, E. R. (1995). Rietveld crystal Structure Refinements, crystal Chemistry and Calculated Powder Diffraction Data for the Polymorphs of Dicalcium Silicate and Related Phases. *Neues Jahrbuch fuer Mineralogie - Abhandlungen* 169, 35–68.

Nguyen, H., Adesanya, E., Ohenoja, K., Kriskova, L., Pontikes, Y., Kinnunen, P., et al. (2019). Byproduct-based Ettringite Binder - A Synergy between Ladle Slag and gypsum. *Construction Building Mater.* 197, 143–151. doi:10.1016/j.conbuildmat.2018.11.165

Pajares, I., de la Torre, Á. G., Martínez-Ramírez, S., Puertas, F., Blanco-Varela, M.-T., and Aranda, M. A. G. (2002). Quantitative Analysis of Mineralized white Portland Clinkers: The Structure of Fluorellestadite. *Powder Diffr.* 17, 281–286. doi:10.1154/1.1505045

Palacios, L., Cabeza, A., Bruque, S., García-Granda, S., and Aranda, M. A. G. (2008). Structure and Electrons in Mayenite Electrides. *Inorg. Chem.* 47, 2661–2667. doi:10.1021/ic7021193

Pelletier, L., Winnefeld, F., and Lothenbach, B. (2010). The Ternary System Portland Cement-Calcium Sulphoaluminate Clinker-Anhydrite: Hydration Mechanism and Mortar Properties. *Cement and Concrete Composites.* 32, 497–507. doi:10.1016/j.cemconcomp.2010.03.010

Puertas, F., Varela, M. T. B., and Molina, S. G. (1995). Kinetics of the thermal Decomposition of C4A3$\bar{S}$ in Air. *Cement Concrete Res.* 25, 572–580. doi:10.1016/0008-8846(95)00046-F

Redhammer, G. J., Tippelt, G., Roth, G., and Amthauer, G. (2004). Structural Variations in the Brownmillerite Series Ca2(Fe2−xAlx)O5: Single-crystal X-ray Diffraction at 25 °C and High-Temperature X-ray Powder Diffraction (25 °C ≤T≤ 1000 °C). *Am. Mineral.* 89, 405–420. doi:10.2138/am-2004-2-322

Ruttanapun, C., Srepusharawoot, P., and Maensiri, S. (2018). Effect of Fe 3+ -doped Ca 12 Al 14 O 33 Cement on Optical and thermal Properties. *Chin. J. Phys.* 56, 252–260. doi:10.1016/j.cjph.2017.12.022

Shame, E. G., and Glasser, F. P. (1987). Stable Ca3SiO5 Solid Solutions Containing Fluorine and Aluminium Made between 1050 and 1250 C. *British Ceramic. Trans. J.* 86, 13–17.

Smith, D. K., and Leider, H. R. (1968). Low-temperature thermal Expansion of LiH, MgO and CaO. *J. Appl. Cryst.* 1, 246–249. doi:10.1107/s0021889868005418

Środek, D., Dulski, M., and Galuskina, I. (2018). Raman Imaging as a New Approach to Identification of the Mayenite Group Minerals. *Sci. Rep.* 8, 13593. doi:10.1038/s41598-018-31809-4

Telschow, S. (2012). *Clinker Burning Kinetics and Mechanism.* Available at: https://orbit.dtu.dk/en/publications/clinker-burning-kinetics-and-mechanism (Accessed February 25, 2021)

Tran, T. T. (2011). *Fluoride Mineralization of Portland Cement: Applications of Double-Resonance NMR Spectroscopy in Structural Investigations of Guest Ions in Cement Phases. PhD Thesis.* Aarhus, Denmark: Interdisciplinary Nanoscience Center, Aarhus University

Tran, T. T., Herfort, D., Jakobsen, H. J., and Skibsted, J. (2009). Site Preferences of Fluoride Guest Ions in the Calcium Silicate Phases of portland Cement from 29Si{19F} CP-REDOR NMR Spectroscopy. *J. Am. Chem. Soc.* 131, 14170–14171. doi:10.1021/ja905223d

Yao, X., Yang, S., Dong, H., Wu, S., Liang, X., and Wang, W. (2020). Effect of CaO Content in Raw Material on the mineral Composition of Ferric-Rich Sulfoaluminate Clinker. *Construction Building Mater.* 263, 120431. doi:10.1016/j.conbuildmat.2020.120431

Zea-Garcia, J. D., de la Torre, A. G., Aranda, M. A. G., and Santacruz, I. (2020). Processing and Characterisation of Standard and Doped Alite-Belite-Ye'elimite Ecocement Pastes and Mortars. *Cement Concrete Res.* 127, 105911. doi:10.1016/j.cemconres.2019.105911

Zea-Garcia, J. D., Santacruz, I., Aranda, M. A. G., and de la Torre, A. G. (2019). Alite-belite-ye'elimite Cements: Effect of Dopants on the Clinker Phase Composition and Properties. *Cement Concrete Res.* 115, 192–202. doi:10.1016/j.cemconres.2018.10.019

Zhmoidin, G. I., and Chatterjee, A. K. (1984). Conditions and Mechanism of Interconvertibility of Compounds 12CaO.7Al2O3 and 5CaO.3Al2O3. *Cement Concrete Res.* 14, 386–396. doi:10.1016/0008-8846(84)90057-7